The 8th European Congress on Computational Methods in Applied Sciences and Engineering
ECCOMAS Congress 2022
5-–9 June 2022, Oslo, Norway

MULTISCALE KINETIC TRANSPORT MODELS FOR THE SPREAD OF EPIDEMICS WITH UNCERTAIN DATA

GIULIA BERTAGLIA[1,2]

[1] Department of Mathematics and Computer Science
University of Ferrara
Via Machiavelli 30, 44121 Ferrara, Italy
e-mail: giulia.bertaglia@unife.it

[2] Istituto Nazionale di Alta Matematica "Francesco Severi"
P.le Aldo Moro 5, 00185 Roma, Italy

Key words: Epidemic Models, Kinetic Transport Models, Hyperbolic Systems, Uncertainty Quantification, Asymptotic-Preserving IMEX Schemes, COVID-19

Abstract. Most epidemiological models are rooted in the pioneering work proposed by Kermack and McKendrick and are based on systems of deterministic ODEs, which describe the temporal evolution of the spread of an infectious disease assuming population and territorial homogeneity. Generally, the concept of the average behavior of a population is sufficient to have a first reliable description of an epidemic development, but the inclusion of the spatial component becomes crucial when it is necessary to consider spatially heterogeneous interventions, as in the case of the COVID-19 pandemic. Moreover, any realistic data-driven model must take into account the large uncertainty in the values reported by official sources such as the amount of infectious individuals. In this work, drawing inspiration from kinetic theory, recent advances on the development of stochastic multiscale kinetic transport models for the spread of epidemics under uncertain data are presented. The propagation of the infectious disease is described by the spatial movement and interactions of individuals divided into commuters moving in the territory on a wide scale and non-commuters acting only on urban scales. The resulting models are solved numerically through a suitable stochastic Asymptotic-Preserving IMEX Runge-Kutta Finite Volume Collocation Method, which ensures a consistent treatment of the system of equations, without loss of accuracy when entering in the stiff, diffusive regime. Application studies concerning the spread of the COVID-19 pandemic in Italy assess the validity of the proposed methodology.

1 INTRODUCTION

The advent of the COVID-19 pandemic has prompted many researchers in the mathematical field and beyond to propose epidemic models increasingly suitable for the study of the evolution of this specific coronavirus, to support the definition of the best strategies for the control of its spread. Most of the proposed models are rooted in the Susceptible–Infected–Removed (SIR) compartmental epidemiological modeling proposed by Kermack and McKendrick [21, 14]. In this deterministic model, which is still widely used, the population is divided into susceptible (S),

who may contract the disease, infected (I), who have already contracted it and may transmit it, and recovered (R), who are either healed (and immune) or deceased. The infectious dynamics is described by a system of ordinary differential equations (ODEs) for the percentages $S(t)$, $I(t)$, $R(t)$ of the population in the three compartments, measured at time $t > 0$, which consider only the temporal evolution of the spread of the epidemic, neglecting the spatial component in favor of an assumption of homogeneity of population and territory [19]. From the classical SIR model, more elaborate models have been introduced to represent the population more realistically, dividing it into further compartments suitable to describe specific characteristic of the infectious disease of interest. Examples of enriched compartmentalizations proposed to study the evolution of the COVID-19 pandemic can be found in [13, 18, 25].

However, such modeling is compromised by some major limitations [1]. On one hand, even though the concept of the average behavior of a population is generally sufficient to have a first reliable description of the development of an epidemic, the homogeneous "mixing" hypothesis does not permit to take into account essential aspects related to the infectious spread, such as the variety of intensity and nature of human contacts based on the age structure of the society [2, 15], the different viral load carried by individuals [16, 23] and the spatial movement of people [4, 11, 17, 29]. Particularly with regard to the latter, the inclusion of the spatial component in epidemiological systems becomes crucial when it is necessary to consider spatially heterogeneous interventions, as was especially needed at the beginning of the COVID-19 pandemic.

On the other hand, the adoption of deterministic models, although more computationally efficient, assumes that initial conditions, boundary conditions and all the parameters involved in the dynamics are known. However, in practical applications, and especially when concerning social sciences, this assumption does not hold true. In the context of epidemic modeling, indeed, initial conditions are certainly affected by uncertainty because data are limited, and screening policy is always a matter of compromises [3, 26].

2 MULTISCALE HYPERBOLIC MODELS OF EPIDEMIC DYNAMICS

In this work, mainly two of the above discussed aspects are addressed through stochastic multiscale kinetic transport models for studying the spread of infectious diseases. These models describe the spatial movement and interactions of a population partitioned (from an epidemiological point of view) on the basis of a chosen compartmental structure and divided into non-commuters, acting only over an urban scale, and commuters moving also on an extra-urban scale, through an appropriate system of partial differential equations (PDEs).

Let us consider initially, for simplicity, the SIR compartmental partitioning [19]. We assume to have a population with individuals having no prior immunity and we neglect the vital dynamics represented by births and deaths because of the time scale considered. To account for the spatial movement of the population, individuals of each compartment are subdivided in three subgroups, $S_{\pm,0}$, $I_{\pm,0}$, $R_{\pm,0}$, traveling in a 1D bounded space domain $\Omega \subseteq \mathbb{R}$ with characteristic speeds $+\lambda_i, -\lambda_i$ and 0 respectively, with $i \in \{S, I, R\}$. Therefore, we consider a stationary part of the population, of non-commuters, characterized by a null characteristic speed. The total compartmental densities are defined as the sum of all the components of the subgroups

$$S = S_+ + S_- + S_0, \qquad I = I_+ + I_- + I_0, \qquad R = R_+ + R_- + R_0\,. \tag{1}$$

Moreover, we introduce the random vector $\mathbf{z} = (z_1, \dots, z_{d_z})^T \in \mathbb{R}^d$ whose components are

assumed to be independent real valued random variables z_k, $k = 1, \dots, d_z$ which characterize possible sources of uncertainty, assuming to know the probability density $p(\mathbf{z}) : \mathbb{R}^{d_z} \to \mathbb{R}_+^{d_z}$ characterizing the distribution of $\mathbf{z}$.

Finding inspiration from the kinetic theory and considering a stochastic framework in which all the epidemic densities depend on $(\mathbf{z}, x, t)$, with $x \in \Omega$ and $t > 0$, we can define the discrete-velocity system of the SIR epidemic transport model of commuting individuals associated to relaxation times τ_i, as

$$\begin{aligned}
\frac{\partial S_\pm}{\partial t} \pm \lambda_S \frac{\partial S_\pm}{\partial x} &= -\frac{\beta_I S_\pm I}{1+\kappa_I I} + \frac{1}{2\tau_S}\left(S_\mp - S_\pm\right), \\
\frac{\partial I_\pm}{\partial t} \pm \lambda_I \frac{\partial I_\pm}{\partial x} &= \frac{\beta_I S_\pm I}{1+\kappa_I I} - \gamma_I I_\pm + \frac{1}{2\tau_I}\left(I_\mp - I_\pm\right), \\
\frac{\partial R_\pm}{\partial t} \pm \lambda_R \frac{\partial R_\pm}{\partial x} &= \gamma_I I_\pm + \frac{1}{2\tau_R}\left(R_\mp - R_\pm\right).
\end{aligned} \tag{2}$$

Here, the parameter $\gamma_I(\mathbf{z}, x, t)$ is the recovery rate of infected (inverse of the infectious period). In the incidence function, $\beta_I(\mathbf{z}, x, t)$ is the transmission rate, which may vary based on the effects of government control actions, such as mandatory wearing of masks, shutdown of specific work/school activities, or full lockdowns [2, 18], while the parameter $\kappa_I(\mathbf{z}, x, t) \geq 0$ acts as incidence damping coefficient based on the self-protective behavior of the individuals that arises from awareness of the risk associated with the epidemic [9, 14].

System (2) is coupled with an ODE SIR model, which describes the evolution of the stationary population of non-commuters:

$$\frac{\mathrm{d}S_0}{\mathrm{d}t} = -\frac{\beta_I S_0 I}{1+\kappa_I I}, \quad \frac{\mathrm{d}I_0}{\mathrm{d}t} = \frac{\beta_I S_0 I}{1+\kappa_I I} - \gamma_I I_0, \quad \frac{\mathrm{d}R_0}{\mathrm{d}t} = \gamma_I I_0. \tag{3}$$

Let us finally observe that, under no inflow/outflow boundary conditions, summing up the equations in (2)-(3) and integrating in the space Ω yields the conservation of the total population, $S + I + R = N$. For the definition of the reproduction number related to this model, the reader can refer to [9].

2.1 Macroscopic formulation and diffusion limit

If we now introduce the macroscopic variables S_c, I_c, R_c for the commuters, with $S_c = S_+ + S_-$, $I_c = I_+ + I_-$, $R_c = R_+ + R_-$, and define the fluxes $J_S = \lambda_S(S_+ - S_-)$, $J_I = \lambda_I(I_+ - I_-)$, $J_R = \lambda_R(R_+ - R_-)$ a hyperbolic model underlying the macroscopic formulation of the spatial propagation of an epidemic at finite speeds, equivalent to the kinetic one presented in system (2), but composed of three equations for the densities,

$$\begin{aligned}
\frac{\partial S_c}{\partial t} + \frac{\partial J_S}{\partial x} &= -\frac{\beta_I S_c I}{1+\kappa_I I}, \\
\frac{\partial I_c}{\partial t} + \frac{\partial J_I}{\partial x} &= \frac{\beta_I S_c I}{1+\kappa_I I} - \gamma_I I_c, \\
\frac{\partial R_c}{\partial t} + \frac{\partial J_R}{\partial x} &= \gamma_I I_c,
\end{aligned} \tag{4}$$

and three equations for the the fluxes,

$$\begin{aligned}
\frac{\partial J_S}{\partial t} + \lambda_S^2 \frac{\partial S_c}{\partial x} &= -\frac{\beta_I J_S I}{1+\kappa_I I} - \frac{1}{\tau_S} J_S \,, \\
\frac{\partial J_I}{\partial t} + \lambda_I^2 \frac{\partial I_c}{\partial x} &= \frac{\lambda_I}{\lambda_S} \frac{\beta_I J_S I}{1+\kappa_I I} - \gamma_I J_I - \frac{1}{\tau_I} J_I \,, \\
\frac{\partial J_R}{\partial t} + \lambda_R^2 \frac{\partial R_c}{\partial x} &= \frac{\lambda_R}{\lambda_I} \gamma_I J_I - \frac{1}{\tau_R} J_R \,,
\end{aligned} \tag{5}$$

is obtained [9]. Note that the above system is coupled with the equations for the non-commuting population (3) through identities (1).

From a formal viewpoint, it can be shown that the proposed model recovers the parabolic behavior expected from standard space-dependent epidemic models in the diffusion limit [9]. In fact, introducing the diffusion coefficients $D_i = \lambda_i^2 \tau_i, i \in \{S, I, R\}$ that characterize the diffusive transport mechanism of S, I, R and letting $\tau_i \to 0$ while keeping the diffusion coefficients finite [22], so entering in the *stiff* region of the system, from (5) we recover Fick's laws,

$$J_S = -D_S \frac{\partial S_c}{\partial x}, \quad J_I = -D_I \frac{\partial I_c}{\partial x}, \quad J_R = -D_R \frac{\partial R_c}{\partial x},$$

which, inserted in (4), lead to the following parabolic reaction-diffusion system for the commuters [4, 24]:

$$\begin{aligned}
\frac{\partial S_c}{\partial t} &= \frac{\partial}{\partial x}\left(D_S \frac{\partial S_c}{\partial x} \right) - \frac{\beta_I S_c I}{1+\kappa_I I} \,, \\
\frac{\partial I_c}{\partial t} &= \frac{\partial}{\partial x}\left(D_I \frac{\partial I_c}{\partial x} \right) + \frac{\beta_I S_c I}{1+\kappa_I I} - \gamma_I I_c \,, \\
\frac{\partial R_c}{\partial t} &= \frac{\partial}{\partial x}\left(D_R \frac{\partial R_c}{\partial x} \right) + \gamma_I I_c \,.
\end{aligned} \tag{6}$$

Therefore, we observe that the relaxation times, together with the characteristic velocities, can modify the nature of the behavior of the solution, which can result either hyperbolic (for small relaxation parameters and finite speeds) or parabolic (when considering relaxation terms that tend to zero and speeds that tend to infinity). This feature of the proposed model makes it particularly suitable for use in describing the dynamics of human populations, which are characterized by movement at different spatial scales. It is therefore natural to assume spatially dependent scaling parameters $\tau_i(x)$ and $\lambda_i(x)$, which reproduce a diffusive dynamics in geographic areas densely populated and a hyperbolic regime in other areas or along the main arteries of communication, avoiding propagation of information at infinite speed over large distances [9, 11].

2.2 Extension to enriched compartmentalizations

The proposed modeling can be potentially extended to any kind of enriched compartmentalization aimed at better analyzing the evolution of the infectious disease under investigation. Here, to account for specific features of the COVID-19, we consider extending the simple SIR

compartmentalization by taking into account two additional epidemic compartments, E and A, resulting in a SEIAR model [5, 8]. Subjects in the E compartment have been exposed to the virus but are still in the latent period, hence result infected but not yet infectious. Furthermore, among the infectious subjects, we distinguish the population between a group of severely symptomatic individuals I and a group of asymptomatic or mildly symptomatic individuals A.

Defining the total density of the additional compartments, $E = E_+ + E_- + E_0$, $A = A_+ + A_- + A_0$, the resulting discrete-velocity system of the SEIAR epidemic transport model for commuters reads

$$\begin{aligned}
\frac{\partial S_\pm}{\partial t} \pm \lambda_S \frac{\partial S_\pm}{\partial x} &= -\frac{\beta_I S_\pm I}{1+\kappa_I I} - \frac{\beta_A S_\pm A}{1+\kappa_A A} + \frac{1}{2\tau_S}\left(S_\mp - S_\pm\right), \\
\frac{\partial E_\pm}{\partial t} \pm \lambda_E \frac{\partial E_\pm}{\partial x} &= \frac{\beta_I S_\pm I}{1+\kappa_I I} + \frac{\beta_A S_\pm A}{1+\kappa_A A} - aE_\pm + \frac{1}{2\tau_E}\left(E_\mp - E_\pm\right), \\
\frac{\partial I_\pm}{\partial t} \pm \lambda_I \frac{\partial I_\pm}{\partial x} &= a\sigma E_\pm - \gamma_I I_\pm + \frac{1}{2\tau_I}\left(I_\mp - I_\pm\right), \\
\frac{\partial A_\pm}{\partial t} \pm \lambda_A \frac{\partial A_\pm}{\partial x} &= a(1-\sigma) E_\pm - \gamma_A A_\pm + \frac{1}{2\tau_A}\left(A_\mp - A_\pm\right), \\
\frac{\partial R_\pm}{\partial t} \pm \lambda_R \frac{\partial R_\pm}{\partial x} &= \gamma_I I_\pm + \gamma_A A_\pm + \frac{1}{2\tau_R}\left(R_\mp - R_\pm\right),
\end{aligned} \tag{7}$$

which is coupled with the following SEIAR model describing the evolution of non-commuting individuals:

$$\begin{aligned}
\frac{\mathrm{d}S_0}{\mathrm{d}t} &= -\frac{\beta_I S_0 I}{1+\kappa_I I} - \frac{\beta_A S_0 A}{1+\kappa_A A}, \\
\frac{\mathrm{d}E_0}{\mathrm{d}t} &= \frac{\beta_I S_0 I}{1+\kappa_I I} + \frac{\beta_A S_0 A}{1+\kappa_A A} - aE_0, \\
\frac{\mathrm{d}I_0}{\mathrm{d}t} &= a\sigma E_0 - \gamma_I I_0, \\
\frac{\mathrm{d}A_0}{\mathrm{d}t} &= a(1-\sigma) E_0 - \gamma_A A_0, \\
\frac{\mathrm{d}R_0}{\mathrm{d}t} &= \gamma_I I_0 + \gamma_A A_0.
\end{aligned} \tag{8}$$

The quantity $\gamma_A(\mathbf{z}, x, t)$ is the recovery rate of asymptomatic/mildly symptomatic infected, which is distinguished from the recovery rate of highly symptomatic infected previously introduced $\gamma_I(\mathbf{z}, x, t)$; $a(\mathbf{z}, x, t)$ represents the inverse of the latency period and $\sigma(\mathbf{z}, x, t)$ is the probability rate of developing severe symptoms [17, 13]. In this model, the transmission of the infection is governed by two different incidence functions, simply to distinguish between the behavior of I and A individuals, where a different contact rate β_A and coefficient κ_A are taken into account for mildly/no symptomatic people.

Let us observe that, similarly to the diffusive scaling presented in Section 2.1 for the SIR-type model, introducing the same definition of flux for the additional compartments, J_E and J_A, we get an analogous macroscopic formulation also for the SEIAR-type transport model. Furthermore, defining also $D_E = \lambda_E^2 \tau_E$ and $D_A = \lambda_A^2 \tau_A$, we recover a parabolic reaction-diffusion SEIAR-type system in the zero-relaxation limit [22]. The reader can refer to [8] for more details on this derivation and for the definition of the reproduction number.

2.3 Extension to network modeling

The multiscale hyperbolic transport models here proposed can be extended to network approaches in the sense of those presented in traffic, chemotaxis or blood flow models [12, 27, 28]. In fact, it is possible to structure a 1D network considering that nodes of the network identify locations of interest (such as municipalities, provinces or, in a wider scale, regions), while arcs represent the ensemble of paths linking each location to the others. The epidemic state of each node will therefore evolve in time influenced by the mobility of the commuters, always considering a part of the population composed by non-commuting individuals remaining at their origin node.

At each arc-node interface, the arising Riemann Problem is solved employing the Riemann Invariants of the system (which corresponds to the kinetic densities), guaranteeing the conservation of fluxes at the interface and ensuring that the global mass (population) of the system is conserved. Details of the implementation are given in [8, 9].

3 NUMERICAL METHOD

To investigate the effects of uncertainties involved in the proposed stochastic multiscale transport models on the solution of the problem, we couple a second-order Implicit-Explicit (IMEX) Runge-Kutta (RK) Finite Volume (FV) method with a stochastic Collocation approach [8]. The Stochastic Collocation method is chosen because of two main advantages:

- it is a *non-intrusive* method which simply requires the evaluation of the solutions of the corresponding deterministic problem at each collocation point and, because of this feature, avoids the loss of important structural properties of the original system (e.g. hyperbolicity, well balancing, positivity);
- it belongs to the class of pseudo-spectral methods that reflect the high accuracy of *generalized Polynomial Chaos* (*gPC*) approaches. Indeed, when the solution possesses sufficient smoothness in the stochastic space, these methods have been proven to achieve an exponential convergence rate and to preserve this accuracy in the diffusive (stiff) limit.

To evaluate the solution at each collocation point, for the time discretization we consider a second-order IMEX RK schemes proposed in [10] for applications to hyperbolic systems with stiff relaxation terms. The chosen scheme benefits from the Asymptotic-Preserving (AP) property, which guarantees that the scheme consistently captures the diffusion limit and that the choice of the time discretization step is not related to the smallness of the scaling parameter τ. At each internal stage of the IMEX RK scheme, we apply a total variation diminishing (TVD) FV method. To achieve second-order accuracy also in space while avoiding the occurrence of spurious oscillations, a classical minmod slope limiter is used.

We remark that, given the non-intrusive nature of the stochastic Collocation method, the AP property of the deterministic IMEX scheme is preserved also in the stochastic framework, leading to a stochastic AP scheme that permits to switch from a stochastic Collocation method for the advection problem to a stochastic Collocation method for the diffusive problem in a uniform way with respect to the involved parameters [20].

For further details regarding the numerical method and the convergence analysis the reader is referred to [6, 8].

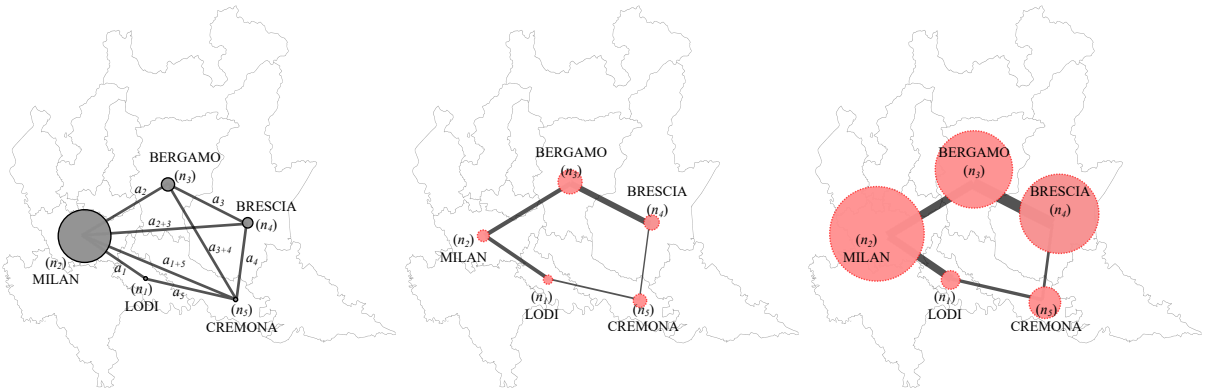

Figure 1: Left: representation of the network of the Lombardy test case, composed of 5 nodes, corresponding to the provinces of interest and 5 arcs, connecting each city to the others, considering all the main paths of commuters. The dimension of the node is proportional to the dimension of the urbanized area of the province. Middle and right: estimated spread of COVID-19 in Lombardy during the first wave of the virus on March 12, 2020 (middle) and March 27, 2020 (right). The radius of the nodes in the network and the width of the arcs is proportional to the amount of total infected individuals, including asymptomatic individuals.

We would like to emphasize that for the stochastic Collocation method to be used, the PDF of the random inputs must be known. Among the various techniques of uncertainty quantification (UQ), the approaches based on stochastic strategies that do not necessarily require the a-priori knowledge of the probability distribution of the uncertain parameters are particularly interesting in view of a comparison with experimental data. We invite the reader to refer to [7] for an example of alternative UQ method based on a Bi-Fidelity approach for multiscale epidemic transport models which efficiently alleviate such a limitation.

3.1 APPLICATION TO THE EMERGENCE OF COVID-19 IN ITALY

To analyze the effectiveness of the proposed approach in a realistic geographical and epidemic scenario, we designed a numerical setting reproducing the evolution of the first outbreak of COVID-19 in the Lombardy Region of Italy, from February 27, 2020 to March 27, 2020, with respect to uncertainties underlying the initial conditions and chosen epidemic parameters.

A five-node network is considered, whose nodes represent the 5 main provinces interested by the epidemic outbreak in the first months of 2020: Lodi (n_1), Milan (n_2), Bergamo (n_3), Brescia (n_4) and Cremona (n_5). The arcs connecting each node to the others identify the main set of routes and railways viable by commuters each day. A schematic representation of this network is shown in Fig. 1 (left).

The characteristic speed associated to each arc is fixed to permit a full round trip in each origin-destination section within a day, while the relaxation time is assigned so that the model recovers a hyperbolic regime. On the other hand, a parabolic setting is prescribed in the cities for commuters in order to correctly capture the diffusive behavior of the disease spread which typically occurs in highly urbanized zones. For the compartment I, we fix $\lambda_I = 0$ in all the nodes of the network, because we assume that all the severely symptomatic individuals are detected and quarantined. The amount of total inhabitants of each province is given by 2019 data of the

Italian National Institute of Statistics. Transmission coefficients at arc-node interfaces as well as percentages of commuters belonging to each province are instead imposed recurring to official national assessment of mobility flow.

For the model calibration, we first solve an optimization least square error (LSE) process using the cumulative number of infected $I(t) + R_I(t)$ reported by the Italian Civil Protection Department, recurring to an SEIAR ODE model for the whole Lombardy Region. In the minimization we fix $\gamma_I = 1/14$, $\gamma_A = 1/7$ and $a = 1/3$ according to [13, 17], as given clinical parameters, and $\sigma = 1/12.5$ as in [13], fixing $\kappa_I = \kappa_A = 30$. We estimate $\beta_A = 0.545$, setting $\beta_I = 0.03\,\beta_A$ as in [13, 17]. Since after February 23, 2020, Codogno city (Lodi), is put under strict lockdown as "red zone", a reduced transmission rate is considered for the node of Lodi, with $\beta_A = 0.500$. With the above setting, we obtain an initial expected value of the reproduction number in the whole network $\mathbb{E}[R_0] = 3.6$ which is in agreement with literature estimations [13, 17]. Subsequent social restrictions have been implemented by suitable reductions of β and increment of κ, as well as changes in the number of commuters (following mobility data tracked by Google GPS systems).

Due to the screening policy adopted in Italy during the first wave of COVID-19, we chose to associate all detected infected individuals to the I compartment, still considering that the tracking of positive individuals cannot be considered exempt from uncertainty. Thus, we introduce a random input $z \sim \mathcal{U}(0,1)$ and define initial conditions for compartment I, at each node, as

$$I(x,0,z) = I^0(1+z)\,, \tag{9}$$

with I^0 density of infectious people on February 27, 2020, as given by data recorded by the Civil Protection Department of Italy. To evaluate the initial condition for the rest of the compartments (excluding removed, being $R(x,0,z) = 0$), the problem is solved prior to February 27, recurring again to an SEIAR ODE model for the whole Lombardy region and imposing an initial condition of one single exposed individual, estimating $E(x,0,z) \approx 10\,I(x,0,z)$ and $A(x,0,z) \approx 9\,I(x,0,z)$, and evaluating for conservation $S(x,0,z) = N(x,0) - E(x,0,z) - I(x,0,z) - A(x,0,z) - R(x,0,z)$. Finally, also β_I is considered a random parameter, with

$$\beta_I(0,z) = \beta_{I,0}\left(1 + \frac{z}{0.06}\right)\,,$$

indicating that the more the number of infected in I increases relative to the observed value, the more the transmission rate of this compartment tends to that of compartment A, proportionally to the error in I. For further details the reader can refer to [8].

4 DISCUSSION AND CONCLUSIONS

Numerical results are reported qualitatively for the whole network in Fig. 1 (middle and right) and quantitatively in Fig. 2 for three representative cities, namely Lodi, Milan, Bergamo, and the whole Lombardy network. In the first column of Fig. 2, the expected evolution in time of each class of infected individuals, together with 95% confidence intervals, is shown. Each plot is also associated with the temporal evolution of the reproduction number $R_0(\mathbf{z}, t)$. One can see the capacity of the model to reproduce a very heterogeneous epidemic trend in the network, highlighting the relevance of taking into account the spatial component in epidemiological

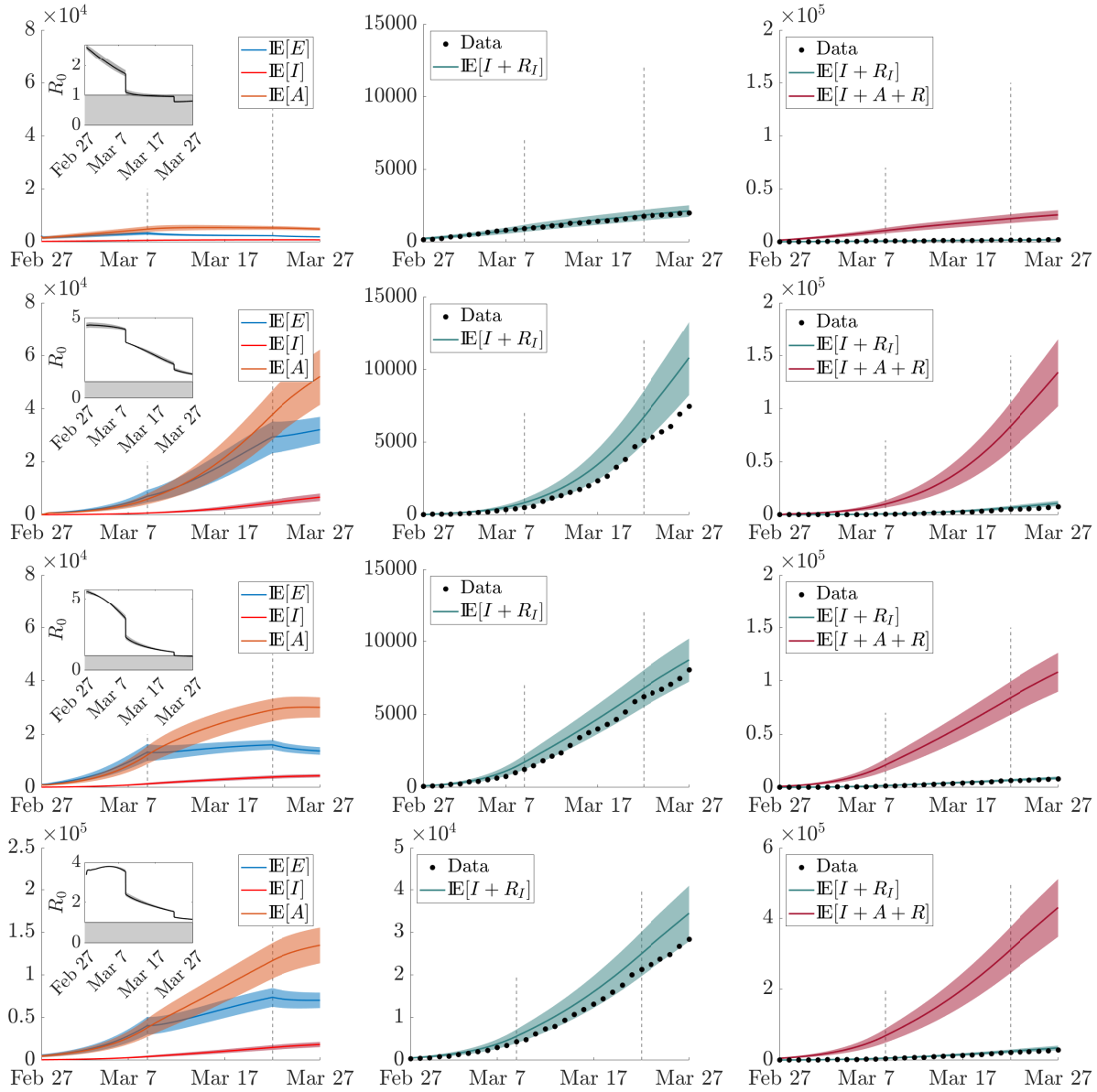

Figure 2: Expected evolution in time, with 95% confidence intervals, for chosen representative cities, Lodi (first row), Milan (second row), Bergamo (third row), and the whole Lombardy network (fourth row), of: compartments E, A, I, together with the basic reproduction number R_0 (left); cumulative amount of severe infectious $(I + R_I)$ compared with data of cumulative infectious taken from the COVID-19 repository of the Civil Protection Department of Italy (middle); cumulative amount of severe infectious $(I+R_I)$ with respect to the effective cumulative amount of total infectious people, including asymptomatic and mildly symptomatic individuals $(I + A + R)$ (right). Vertical dashed lines identify the onset of governmental lockdown restrictions.

models. The agreement between the evolution of the reproduction number and the epidemic spread can also be observed. In particular, it is confirmed the decline of the daily number of

infected as R_0 reaches values below 1, as shown in the plots for Lodi (first row) and Bergamo (third row). On the other hand, the persistence of the virus in the complete network (last row), and especially in Milan (second row), is noticed until the last day of the simulation, where the reproduction number remains greater than 1.

As visible from the second column in Fig. 2, the lower bound of the confidence band of the cumulative amount in time of the severely symptomatic individuals is comparable with the observed data of the Civil Protection Department of Italy. As expected, the mean value of infected people is higher, especially in Milan (the province most affected by the virus during the beginning of the pandemic), due to the uncertainty of available data.

The comparison between the expected evolution in time of the cumulative amount of I with respect to the effective cumulative amount of total infectious people, including also compartment A, is shown in the third column of Fig. 2. Here, it can be noticed how much of the spread of COVID-19 has actually been lost from the observed data during the first outbreak and the impact that the presence of asymptomatic or undetected subjects has had on the epidemic evolution.

REFERENCES

[1] Albi, G. et al. Kinetic modelling of epidemic dynamics: social contacts, control with uncertain data, and multiscale spatial dynamics. In: *Predicting Pandemics in a Globally Connected World*, Birkhauser-Springer Series Modeling and Simulation in Science, Engineering and Technology. Springer-Nature, Vol. 1 (2022).

[2] Albi, G., Pareschi, L., and Zanella, M. Control with uncertain data of socially structured compartmental models. *J. Math. Biol.* (2021) **82**:63.

[3] Albi, G., Pareschi, L., and Zanella, M. Modelling lockdown measures in epidemic outbreaks using selective socio-economic containment with uncertainty. *Math. Biosci. Eng.* (2021) **18**(6):7161–7190.

[4] Berestycki, H., Roquejoffre, J.M., and Rossi, L. Propagation of Epidemics Along Lines with Fast Diffusion. *Bull. Math. Biol.* (2021) **83**:2.

[5] Bertaglia, G., Boscheri, W., Dimarco, G., and Pareschi, L. Spatial spread of COVID-19 outbreak in Italy using multiscale kinetic transport equations with uncertainty. *Math. Biosci. Eng.* (2021) **18**(5):7028–7059.

[6] Bertaglia, G., Caleffi, V., Pareschi, L., and Valiani, A. Uncertainty quantification of viscoelastic parameters in arterial hemodynamics with the a-FSI blood flow model. *J. Comp. Phys.* (2021) **430**:110102.

[7] Bertaglia, G., Liu, L., Pareschi, L., and Zhu, X. Bi-fidelity stochastic collocation methods for epidemic transport models with uncertainties. *Netw. Heterog. Media* (2022) **17**(3):401–425.

[8] Bertaglia, G. and Pareschi, L. Hyperbolic compartmental models for epidemic spread on networks with uncertain data: Application to the emergence of Covid-19 in Italy. *Math. Models Methods Appl. Sci.* (2021) **31**(12):2495–2531.

[9] Bertaglia, G. and Pareschi, L. Hyperbolic models for the spread of epidemics on networks: Kinetic description and numerical methods. *ESAIM: Math. Model. Numer. Anal.* (2021) **55**:381–407.

[10] Boscarino, S., Pareschi, L., and Russo, G. A unified IMEX Runge-Kutta approach for hyperbolic systems with multiscale relaxation. *SIAM J. Numer. Anal.* (2017) **55**(4):2085–2109.

[11] Boscheri, W., Dimarco, G., and Pareschi, L. Modeling and simulating the spatial spread of an epidemic through multiscale kinetic transport equations. *Math. Models Methods Appl. Sci.* (2021) **31**(6):1059–1097.

[12] Bretti, G., Natalini, R., and Ribot, M. A hyperbolic model of chemotaxis on a network: a numerical study. *ESAIM: Math. Model. Numer. Anal.* (2014) **48**(1):231–258.

[13] Buonomo, B. and Della Marca, R. Effects of information-induced behavioural changes during the COVID-19 lockdowns: The case of Italy: COVID-19 lockdowns and behavioral change. *R. Soc. Open Sci.* (2020) **7**:201635.

[14] Capasso, V. and Serio, G. A generalization of the Kermack-McKendrick deterministic epidemic model, *Math. Biosci.* (1978) **42**:43–61.

[15] Colombo, R. M., Garavello, M., Marcellini, F., and Rossi, E. An age and space structured SIR model describing the Covid-19 pandemic. *J. Math. Ind.* (2020) **10**:22.

[16] Della Marca, R., Loy, N., and Tosin, A. An SIR–like kinetic model tracking individuals' viral load. *Netw. Heterog. Media* (2022) **17**(3):467.

[17] Gatto, M. et al. Spread and dynamics of the COVID-19 epidemic in Italy: Effects of emergency containment measures. *PNAS* (2020) **117**(19):10484–10491.

[18] Giordano, G. et al. Modelling the COVID-19 epidemic and implementation of population-wide interventions in Italy. *Nat. Med.* (2020) **26**:855–860.

[19] Hethcote, H.W. The Mathematics of Infectious Diseases. *SIAM Rev.* (2000) **42**(4):599–653.

[20] Jin, S., Xiu, D., and Zhu, X. Asymptotic-preserving methods for hyperbolic and transport equations with random inputs and diffusive scalings. *J. Comput. Phys.* (2015) **289**:35–52.

[21] Kermack W. O. and McKendrick, A. G. A contribution to the mathematical theory of epidemics. *Proc. R. Soc. London. Ser. A* (1927) **115**(772):700–721.

[22] Lions, P. L. and Toscani, G. Diffusive limit for finite velocity Boltzmann kinetic models. *Rev. Mat. Iberoam.* (1997) **13**(3):473–513.

[23] Loy, N. and Tosin, A. A viral load-based model for epidemic spread on spatial networks. *Math. Biosci. Eng.* (2021) **18**(5):5635–5663.

[24] Murray, J. D. *Mathematical Biology II: Spatial Models and Biomedical Applications*, 3rd ed., Springer-Verlag (2003).

[25] Parolini, N. et al. SUIHTER: a new mathematical model for COVID-19. Application to the analysis of the second epidemic outbreak in Italy. *Proc. R. Soc. A: Math. Phys. Eng. Sci.* (2021) **477**(2253):20210027.

[26] Piazzola, C., Tamellini, L., and Tempone, R. A note on tools for prediction under uncertainty and identifiability of SIR-like dynamical systems for epidemiology. *Math. Biosci.* (2021) **332**:108514.

[27] Piccioli, F., Bertaglia, G., Valiani, A., and Caleffi, V. Modeling blood flow in networks of viscoelastic vessels with the 1-D augmented fluid–structure interaction system. *J. Comput. Phys.* (2022) **464**:111364.

[28] Piccoli, B. and Garavello, M. *Traffic Flow on Networks.* American Institute of Mathematical Sciences (2006).

[29] Viguerie, A. et al. Simulating the spread of COVID-19 via a spatially-resolved susceptible–exposed–infected–recovered–deceased (SEIRD) model with heterogeneous diffusion. *Appl. Math. Lett.* (2021) **111**:106617.